Impact of Passband Shift in Optical Wireless Communication Systems based on Wavelength Division

Giovanni Luca Martena
Research Dept.
pureLiFi Ltd.
Edinburgh, United Kingdom

Rui Bian
Research Dept.
pureLiFi Ltd.
Edinburgh, United Kingdom

Harald Haas
Dept. of Electrical and Electronic Engineering
University of Strathclyde
Glasgow, United Kingdom

***Abstract*—In this paper we investigate the impact of the passband shift (PS) phenomenon on optical wireless communication (OWC) systems based on wavelength division (WD). We first introduce the associated challenges, then we discuss the mathematical framework needed to evaluate the performance of systems based on WD when the impact of the PS phenomenon is taken into account. We introduce the concept of spectral overlap (SO) and discuss its role in the design of WD solutions. Results show that this design phase has to take the SO into account, and that its careful balance with the channel gain is essential when multiple colours are used for parallel communication in OWC.**

***Index Terms*—wavelength division, OFs, lifi, iot**

I. Introduction

Optical wireless communication (OWC) is becoming a more and more mature technology, and is now a widely recognised complement to radiofrequency (RF) communication systems. Moreover, the Internet of Things (IoT) and its applications form a good match with OWC and Light Fidelity (LiFi) [1]–[6] because of its vast amount of additional spectral resources, inherent security and lack of cables that are a hindrance in massive and dense deployments. OWC uses visible light, through a grid of lighting fixtures that act as Access Points (APs) to deliver both communication and illumination functionalities at the same time. Wavelength division (WD) is a promising framework for doing this, as the use of multiple colours not only allows the implementation of Smart Lighting functionalities, but also to use colour as an additional degree of freedom, and a way to achieve channel separation. Additionally, these light sources are not based on phosphor-based colour conversion to produce white light. In fact, the phosphor reduces their frequency response and hence the available data rates. WD avoids this fundamental limitation. A practical implementation of WD uses multiple colours at transmitter side, paired with as many thin-film optical filters (OFs) at receiver side. These OFs suffer from the PS phenomenon, which causes a shift of an OF spectrum towards shorter wavelengths. This can impair the quality of the signal in a potentially strong capacity. As a consequence, one of the major challenges to supporting full user mobility in WD systems is the PS phenomenon. There is a specific line of research tackling user mobility characteristics, and an important result in this regard is the work in [7]. More specifically, it provides an analytical approximation of the Probability Density Function (PDF) of the angle of inclination of a mobile device.

Based on these findings, the key contributions of this work can be summarised as follows:

- Starting from the aforementioned previous works, we use the existing closed form approximation of the cosine of the angle of incidence (AoI) of a portable device used in portrait mode during walking activities, with respect to a light source, to derive a closed form approximation of the PDF of the central wavelength (CWL) of an OF at its receiver including the PS effect. Then, we validate this new approximation with Monte-Carlo simulations.
- We write a formal definition of the spectral overlap (SO) parameter, which takes both the AoI and PS into account.
- We discuss how this knowledge can be used in the system design phase for a WD-based LiFi network.

The rest of this paper is organised as follows: in Section II the state of the art is presented. This includes a discussion around the key aspects of LiFi, IoT, WD and the impact of the PS phenomenon. In Section III the research challenges are introduced. In Section IV, the closed form approximation of the shifted CWL for a mobile device during walking activities is derived first, then the concept of the SO is presented, and its impact on OWC and LiFi systems employing WD is discussed. In Section V the simulation results are presented. Section VI contains the conclusions and outlines possible directions for future work.

II. State of the Art

A. LiFi

Visible light communication (VLC) is an OWC technology that makes use of Light Emitting Diodes (LEDs) or Laser Diodes (LD) to transmit a signal by means of Intensity Modulation/Direct Detection (IM/DD) to a Photo Detector (PD). LiFi is a further step. In fact, it is a multipoint wireless communication network, in which each LED can be used as

an AP in a dense deployment providing connectivity to many users simultaneously [8]. As LiFi allows for very small cells arranged in a dense deployment, this is also referred to as an atto-cellular wireless network [9].

B. IoT

IoT is a communication framework that allows many everyday objects and devices featuring various kinds of sensors, software and other technologies, to become nodes of a network, with the purpose of gathering and sharing different kinds of data and communicating over the Internet [10].

In this context, LiFi is seen as an enabler for the IoT [1]–[5].

C. Wavelength Division

Wavelength division multiplexing (WDM) and wavelength division multiple access (WDMA) are both WD paradigms. The use of colour as an additional degree of freedom in OWC is promising because it allows a good degree of separation over multiple channels (usually 3 or 4). This is achieved in this work with a combination of red (R), green (G), blue (B) and amber (A) LEDs at the transmitter and an equal number of PDs with matching coloured OFs at the receiver, thus improving the network capacity. This general approach has been demonstrated successfully in several instances, such as [11], [12]. In fact, even with off the shelf components not specifically designed for OWC, the ability of using colours as additional parallel channels in WDM increases the network capacity, with the highest reported being 15.74 GBps. This comes at the cost of a higher number of components in the frontend, since the number of receivers on each device has to match the number of colours available. Another benefit is that this paradigm is independent of the employed modulation scheme, as each colour can be seen as an individual separate channel. WDMA [13] employs a similar system to that of WDM. The key difference is that in WDMA each colour is meant to serve a different user, thus providing a tradeoff between the number of serviceable users (which increases with the number of available channels) and the maximum achievable data rate for each user. In our previous work, a novel adaptive WDMA channel allocation scheme for a densely deployed LiFi network has been proposed, tested with Monte Carlo simulations, and compared with a state-of-the-art fixed WDMA. Results have shown that for mobile users in walking activities, if using adaptive WDMA, it is possible to reduce the probability of link outage from an average of 31.25% to only 0.72%. Moreover, when using a simple modulation scheme like on-off keying (OOK), the average achievable data rate of 106 Mbps is achieved with adaptive WDMA as opposed to 77 Mbps when using state-of-the-art WDMA [14]. It has to be noted though that for both WDM and WDMA, spectral leakage can lead to severe cross-talk if the receiver design is not carefully considered, especially in terms of choosing the right OFs [15]–[17].

III. Research Challenges

The impact of the random orientation of devices is of crucial importance in OWC and LiFi because it is linked with performance stability, and has recently drawn attention. In [7] the authors have carried out experimental measurements and found that, in walking activities, the inclination angle at which a mobile device is held (θ) follows a Gaussian distribution with a mean of 29.67° and a standard deviation of 7.68°. In [18]–[21] the impact of random orientation on the performance of OWC and LiFi systems has been investigated. Another important consequence of random orientation, which is especially relevant to WD-based OWC and LiFi systems, comes from the PS phenomenon. It consists of a shift towards shorter wavelengths of the relative transmission spectra of such OFs, with a dependence on the AoI of the impinging light. The shifted CWL of an OF, $\lambda_{\mathrm{OF}}(\psi)$, is dependent on the AoI of the impinging light, and is given in [22]:

$$\lambda_{\mathrm{OF}}(\psi) = \lambda_{\mathrm{OF}}(\psi = 0)\sqrt{1 - \frac{\sin^2(\psi)}{n_{\mathrm{e}}^2}} \tag{1}$$

where ψ is the AoI of the impinging light, $\lambda_{\mathrm{OF}}(\psi = 0)$ is the CWL of the considered transmission spectrum when the light hits the receiver perpendicularly (that is, when $\psi = 0$), and n_{e} is the effective refractive index of the specific OF employed. It is clear from equation 1 that if $\psi \neq 0$ the transmission spectrum of the OF will be shifted towards shorter wavelengths. This is bound to become a major limitation to the channel separation capabilities of systems that employ WD. The reason is that many kinds of portable devices (such as smartphones and wearables) are not designed to be used at a fixed angle. Moreover, even appliances not designed for mobile use (such as smart TVs, or industrial machines) will not always be placed with an optimal AoI with respect to the APs, due to various spatial constraints that might occur.

IV. Mathematical Framework

A. Approximation of the CWL of a shifted OF spectrum

In order to evaluate the performances of a system employing WD in the presence of the PS phenomenon, we can rely on the user movement statistics presented in [7]. In this work we are going to specifically focus on the device's polar angle, θ, which describes the inclination at which the user is holding the device in order to keep good visibility during its use in portrait mode. This is shown, along with the system geometry, in Fig. 1.

For the rest of the paper, we will refer to "AP 1" as the AP right above the user, and to "AP 2" as the AP that is displaced by a distance d' with respect to AP 1. The mobile device is at a distance d_1 and d_2 from AP 1 and AP 2, respectively, and the unit vector $\boldsymbol{n}'_{\mathrm{u}}$ is perpendicular to the receiver's surface. The polar angle of the device θ influences directly the AoIs, ψ_1 and ψ_2. Regarding user mobility the authors of [7] report that the cosine of ψ follows a truncated Gaussian distribution, if the users are walking, and a truncated Laplace distribution, if the users are sitting.

Throughout this paper only the walking scenario is considered, as accounting for user mobility is a major challenge in LiFi. In [7] an approximation of the Probability Density

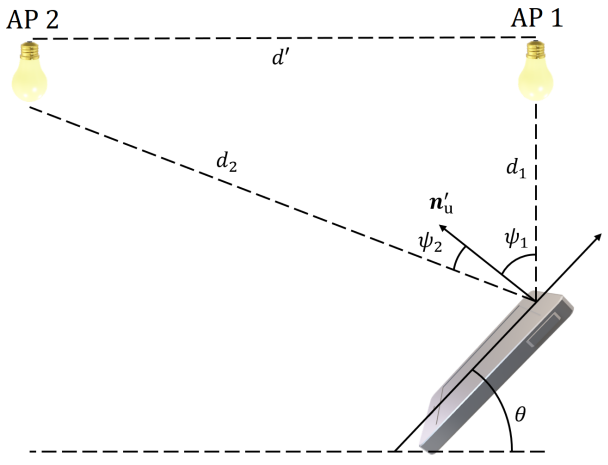

Fig. 1. System geometry. The 2 APs are labeled as "AP 1" and "AP 2". The angles of incidence ψ for AP 1 and 2, and the polar angle θ, are shown. Note that in this work, the polar angle describes the inclination of the device when used in portrait mode.

Function (PDF) of $\cos\psi$ based on the first-order Taylor series ($\sin\theta \cong \theta'$ and $\cos\theta \approx 1$) is given as:

$$f_{\cos\psi}(\hat{\psi}) \approx \frac{\sqrt{2}e^{-\frac{1}{2}\left(\frac{\hat{\tau}-\hat{\mu}_\theta}{\hat{\sigma}_\theta}\right)^2}}{\hat{\sigma}_\theta\sqrt{\pi}[\mathrm{erf}\left(\frac{\hat{\tau}_{\max}-\hat{\mu}_\theta}{\sqrt{2}\hat{\sigma}_\theta}\right) - \mathrm{erf}\left(\frac{\hat{\tau}_{\min}-\hat{\mu}_\theta}{\sqrt{2}\hat{\sigma}_\theta}\right)]} \tag{2}$$

With $\hat{\tau}_{\min} \leq \hat{\tau} \leq \hat{\tau}_{\max}$. Here, $\hat{\tau}$ denotes the realisation of the Random Variable (RV) $\cos\psi$. Moreover, $\hat{\tau}_{\max}$ and $\hat{\tau}_{\min}$ identify the support range of $\hat{\tau}$ (and are not necessarily 0 and 1 as demonstrated in [7]), while $\hat{\mu}_\theta$ and $\hat{\sigma}_\theta$ are respectively the mean and standard deviation of the distribution of the polar angle, θ. Note that this expression is an approximated analytical expression for the PDF, conditioned on the position and orientation of the user. As a consequence, the AoI ψ strictly depends on the polar angle θ).

As is widely recognised, the expression of the geometrical channel gain, $H_{\mathrm{LOS}}(0)$, was formally defined in [23]. A closed form approximation of the PDF and CDF of this parameter have been derived in [7], and respectively given as:

$$f_H(\bar{h}) \approx \frac{1}{h_{\mathrm{n}}} f_{\cos\psi}\left(\frac{\bar{h}}{h_{\mathrm{n}}}\right) + F_{\cos\psi}(\cos\Psi_{\mathrm{c}})\delta(\bar{h}) \tag{3}$$

$$F_H(\bar{h}) \approx F_{\cos\psi}\left(\frac{\bar{h}}{h_{\mathrm{n}}}\right) + F_{\cos\psi}(\cos\Psi_{\mathrm{c}})\mathcal{U}(\bar{h}) \tag{4}$$

With $h_{\min} \leq \bar{h} \leq h_{\max}$. Here $h_{\mathrm{n}} = \frac{(m+1)Ah^m}{2\pi d^{m+2}}$ is a normalisation factor, Ψ_{c} is the half-FOV angle of the receiver, and $F_{\cos\psi}(\cos\Psi_{\mathrm{c}})$ is the closed form expression for the approximated Cumulative Distribution Function (CDF) of $\cos\psi$. Inside h_{n}, m is the Lambertian emission order, A is the detector effective area and d is the distance between the transmitter and the receiver. The $\delta(\bar{h})$ and $\mathcal{U}(\bar{h})$ are the delta Dirac function and the unit step function, respectively.

Starting from (2), it is possible to exploit the fundamental relation $\sin\psi = \sqrt{1-\cos\psi^2}$ and find an expression for the CDF of $\sin\psi$:

$$F_{\sin\psi}(\hat{\eta}) = \Pr\{\sin\psi \leq \hat{\eta}\} = \Pr\{\sqrt{1-\cos\psi^2} \leq \hat{\eta}\}$$

$$F_{\sin\psi}(\hat{\eta}) = 1 - F_{\cos\psi}(\sqrt{1-\hat{\eta}^2})$$

where $\hat{\eta}$ denotes the realisation of the RV $\sin\psi$. This is an important step, as the shift of the CWL of an OF as a result of the PS effect depends on the sine of the AoI. It is then possible to note that:

$$F_{\cos\psi}(\sqrt{1-\hat{\eta}^2}) = \int_0^{\sqrt{1-\hat{\eta}^2}} f_{\cos\psi}(t)\,dt$$

After solving the integral, the closed form CDF of the sine of the AoI can be found:

$$F_{\sin\psi}(\hat{\eta}) = 1 - \frac{1}{U}[\mathrm{erf}\left(\frac{\sqrt{1-\hat{\eta}^2}-\hat{\mu}_\theta}{\sqrt{2}\hat{\sigma}_\theta}\right) + \mathrm{erf}\left(\frac{\hat{\mu}_\theta}{\sqrt{2}\hat{\sigma}_\theta}\right)] \tag{5}$$

and here:

$$U = \mathrm{erf}\left[\frac{\hat{\tau}_{\max}-\hat{\mu}_\theta}{\sqrt{2}\hat{\sigma}_\theta}\right] - \mathrm{erf}\left[\frac{\hat{\tau}_{\min}-\hat{\mu}_\theta}{\sqrt{2}\hat{\sigma}_\theta}\right]$$

Then obtaining the PDF of the sine of the AoI can be achieved by differentiating (5) with respect to $\hat{\eta}$:

$$f_{\sin\psi}(\hat{\eta}) = \frac{d}{d\hat{\eta}}F_{\sin\psi}(\hat{\eta}) = \frac{\sqrt{2}\hat{\eta}e^{-\frac{1}{2}\left(\frac{\sqrt{1-\hat{\eta}^2}-\hat{\mu}_\theta}{\hat{\sigma}_\theta}\right)^2}}{\sqrt{\pi}\hat{\sigma}_\theta U\sqrt{1-\hat{\eta}^2}} \tag{6}$$

Having found an expression of the PDF of the sine of the AoI, it is then possible to realise, by looking at (1), to rewrite it as $\frac{\lambda_{\mathrm{OF}}(\psi)}{\lambda_{\mathrm{OF}}(\psi=0)} = \sqrt{1-\frac{\sin^2(\psi)}{n_{\mathrm{e}}^2}}$ and define a new parameter:

$$\rho(\psi) \triangleq \frac{\lambda_{\mathrm{OF}}(\psi)}{\lambda_{\mathrm{OF}}(\psi=0)} = \sqrt{1-\frac{\sin^2(\psi)}{n_{\mathrm{e}}^2}} \tag{7}$$

This is called spectral displacement and it is the quantity that has to be multiplied by the CWL of the OF that was chosen in the system design phase, $\lambda_{\mathrm{OF}}(\psi=0)$, to obtain the shifted CWL, $\lambda_{\mathrm{OF}}(\psi)$ for a generic AoI. Its support range is $0 \leq \rho(\psi) \leq 1$. By looking at (7) it can be easily verified that if $\psi = 0$, then the normal unit vector of the receiver $\boldsymbol{n}'_{\mathrm{u}}$ is pointing directly towards the transmitter. This means that $\rho(\psi) = 1$, and thus $\lambda_{\mathrm{OF}}(\psi) = \lambda_{\mathrm{OF}}(\psi=0)$. From here, by applying the same steps as (2) and (5), it is possible to consider the PDF of $\sin\psi$ and write a closed form expression for the CDF of the spectral displacement ρ:

$$F_\rho(\hat{\rho}) = 1 - \frac{1}{U}[\mathrm{erf}\left(\frac{1-\hat{\mu}_\theta}{\sqrt{2}\hat{\sigma}_\theta}\right) - \mathrm{erf}\left(\frac{\sqrt{1-n_{\mathrm{OF}}^2(1-\hat{\rho}^2)}-\hat{\mu}_\theta}{\sqrt{2}\hat{\sigma}_\theta}\right)] \tag{8}$$

Here $\hat{\rho}$ is the realisation of the RV $\rho(\psi)$. Differentiation with respect to $\hat{\rho}$ yields the PDF of the ρ parameter:

$$f_\rho(\hat{\rho}) = \frac{\sqrt{2} n_{\text{OF}}^2 \hat{\rho} e^{-\frac{1}{2}\left(\frac{\sqrt{1-\hat{\eta}^2}-\hat{\mu}_\theta}{\hat{\sigma}_\theta}\right)^2}}{\sqrt{\pi}\hat{\sigma}_\theta U \sqrt{1-n_{\text{OF}}^2(1-\hat{\rho}^2)}} \tag{9}$$

It is then possible to exploit the definition of $\rho(\psi)$ and its linearity with respect to $\lambda_{\text{OF}}(\psi)$, and find:

$$F_\lambda(\hat{\lambda}_{\text{OF}}) = F_\rho\left(\frac{\hat{\lambda}_{\text{OF}}}{\lambda_{\text{OF}}(\psi=0)}\right) = \frac{1}{\lambda_{\text{OF}}(\psi=0)} F_\rho(\hat{\rho}) \tag{10}$$

$$f_\lambda(\hat{\lambda}_{\text{OF}}) = f_\rho\left(\frac{\hat{\lambda}_{\text{OF}}}{\lambda_{\text{OF}}(\psi=0)}\right) = \frac{1}{\lambda_{\text{OF}}(\psi=0)} f_\rho(\hat{\rho}) \tag{11}$$

Equations (10) and (11) are the approximated closed form expressions of the CDF and PDF respectively, for the CWL of an OF. These results are inclusive of the PS effect, and are conditioned on the user's location and facing direction.

B. The spectral overlap

The SO, $W(\psi)$, can be defined as:

$$W(\psi) = \begin{cases} 0 & \text{if } \frac{|\lambda_{\text{OF}}(\psi)-\lambda_{\text{LED}}|}{2\Delta\lambda} > 1 \\ 1 - \frac{|\lambda_{\text{OF}}(\psi)-\lambda_{\text{LED}}|}{2\Delta\lambda} & \text{if } 0 < \frac{|\lambda_{\text{OF}}(\psi)-\lambda_{\text{LED}}|}{2\Delta\lambda} \leq 1 \\ 1 & \text{if } \lambda_{\text{OF}}(\psi) = \lambda_{\text{LED}} \end{cases} \tag{12}$$

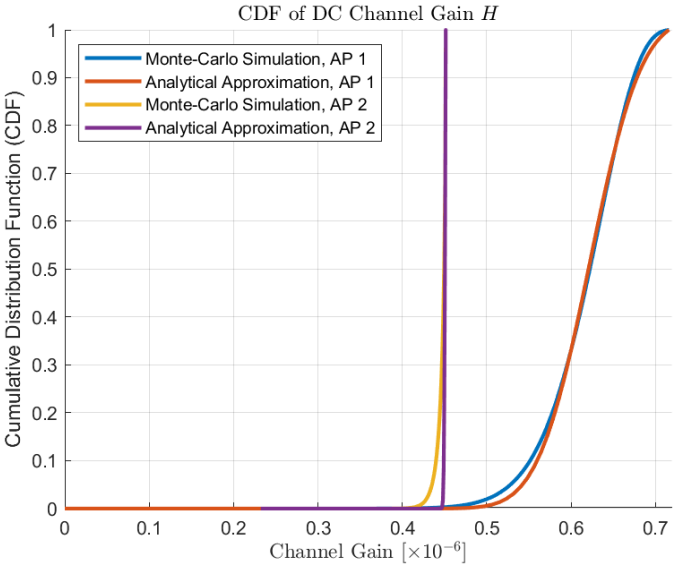

Fig. 2. Monte Carlo simulations VS Analytical Approximation comparison of the CDF of channel gain for AP 1 and 2.

It has to be noted that a closed form approximation of the PDF and CDF for the SO effect is the subject of future work. The SO is meant to represent a measure of the goodness of the overlap between a transmitter and a receiver spectra. If, at a certain AoI, these have the same CWL and width, then they overlap completely and the signal power for that particular channel is maximised.

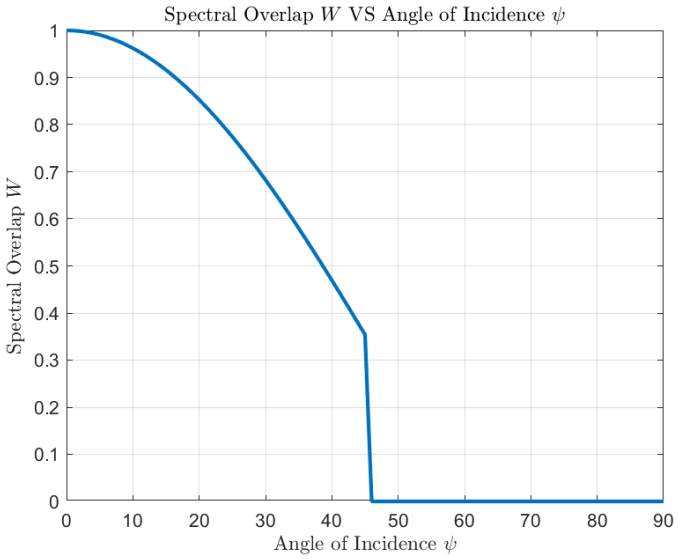

Fig. 3. Spectral overlap W as a function of the AoI, ψ. If the CWLs of the light source and the OF coincide by system design, $W(\psi)$ is a decreasing function of ψ. The discontinuity at $\psi = 45°$ is a result of the receiver FOV.

V. Simulation Results

The simulation scenario is shown in Fig. 1, and can be described as follows. We consider 2 neighbouring APs in a LiFi network, namely AP 1 and AP 2, and one mobile user. This user has a fixed position (right under AP 1) and facing direction (which is opposite to the horizontal component of the unit vector $\boldsymbol{n}'_{\text{u}}$), but holds the mobile device at a variable polar angle θ. We model the emission spectrum of one single-colour LED with a rectangular function centered at $\lambda_{\text{LED}} = 500$ nm with a half-width at half maximum (HWHM) $\Delta\lambda = 25$ nm. A similar function is used to model the OF transmission spectrum with $\lambda_{\text{OF}}(0) = 500$ nm and the same HWHM. This means that the full width of the spectrum is of 50 nm, as is common for many off-the-shelf OFs not specifically designed for OWC. In this work we only consider one of the possible transmitter-receiver colour combinations, as the methodology can readily be extended to any other colours of a WD-based communication system, simply by changing the values of λ_{LED} and $\lambda_{\text{OF}}(0)$. For the OF, we assume an effective refractive index of $n_{\text{OF}} = 1.8$, as this parameter usually ranges between 1.6 and 2.0 for off-the-shelf components. Furthermore, this particular value was used in [22]. We generate 10^6 realizations of θ according to the Gaussian distribution reported in [7]. Then, we calculate the corresponding results for ψ_1, ψ_2, $H_{\text{LOS}}(0)$, $\lambda_{\text{OF}}(\psi)$, and $W(\psi)$ for each realization of θ. At this point we compare these simulation results with the analytical approximations for both the channel gain and the CWL, the first presented in [7] and the second derived throughout Section IV A. Then we show the CDF of the SO, with fitting Gaussian distributions, and discuss all these results. All the simulation parameters are given in Table I.

Fig. 2 shows the first comparison, between Monte Carlo simulations and the analytical approximation of the CDF of

the channel gain given in Equation 4 for both the APs that are being considered in this work. As expected, the channel gain is higher for AP 1 because of its lower distance from the user. In WD-based systems though, the AoI is also influencing the signal strength through the presence of the PS effect. In this regard, calculating the SO of the system for specific AoIs can help a system designer formulate a more accurate link budget that also takes these effects into account.

TABLE I
PARAMETERS

System Parameters		
Symbol	**Description**	***Value***
N	Number of realizations	10^6
d'	Inter-AP distance	1.2 m
A	Single detector area	9 mm^2
Ψ_c	Receiver half Field of View	45°
$\hat{\mu}_\theta$	Mean of polar angle	29.67°
$\hat{\sigma}_\theta$	Standard deviation of polar angle	7.78°
λ_{LED}	LED Central Wavelength	500 nm
n_{OF}	Effective Refractive Index of the OF	1.8
$\Delta\lambda$	LED and OF HWHM	25 nm

TABLE II
RESULTS OF MONTE CARLO SIMULATIONS

	AP 1	**AP 2**
Mean DC Channel Gain	−62.1 dB	−63.5 dB
Mean Spectral Overlap	0.60	0.97
Result Overall Gain	−64.3 dB	−63.6 dB

By considering the analytical expression for the SO provided in (12) plotted in Fig. 3 for AP 1 and increasing ψ, it can be seen that the SO is a decreasing function of ψ, if $\lambda_{\text{OF}}(\psi = 0) = \lambda_{\text{LED}}$.

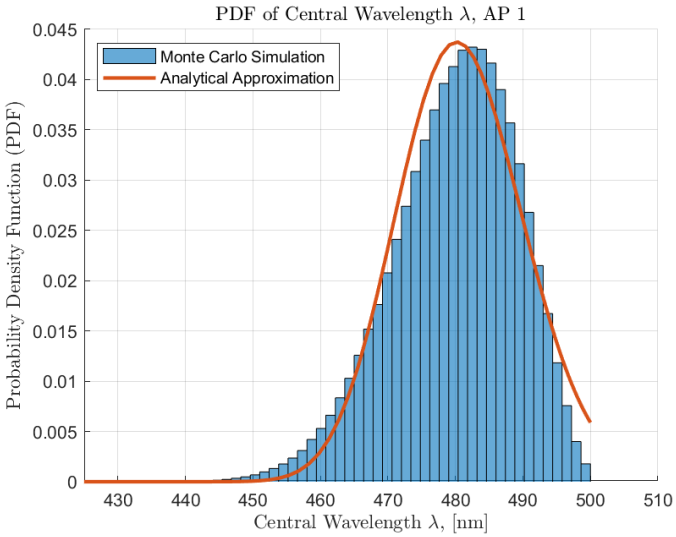

Fig. 4. Monte Carlo simulations VS Analytical Approximation comparison of the PDF of the CWL of the OF for AP 1.

Fig. 4 and 5 show a comparison between Monte Carlo simulations and the analytical approximation of the CWL of

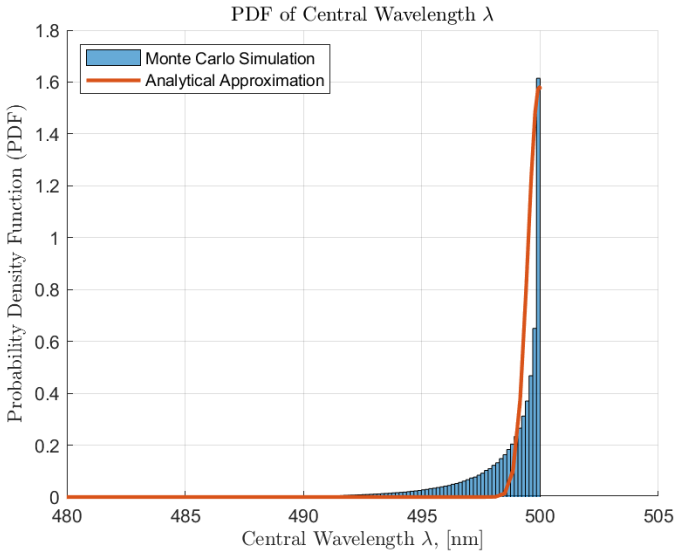

Fig. 5. Monte Carlo simulations VS Analytical Approximation comparison of the PDF of the CWL of the OF for AP 2.

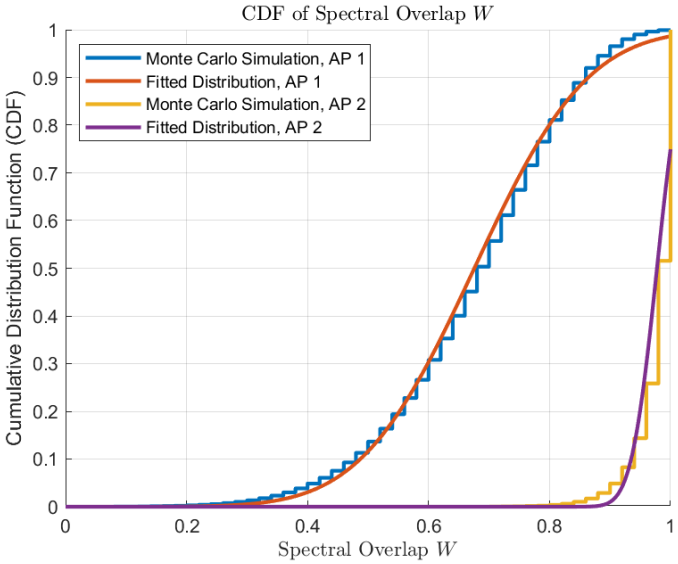

Fig. 6. CDF of the SO for both APs, obtained with Monte Carlo simulations, and fitted Gaussian Distributions. Despite being right below AP 1, the SO is maximised for AP 2 because the mean of the polar angle θ makes the device face AP 2.

the OF, $\lambda_{\text{OF}}(\psi)$, derived in (11). The CWL distribution is much more centered towards the original $\lambda_{\text{OF}}(\psi = 0)$ choice for AP 2 than it is for AP 1, due to the angle at which the user is holding the device (θ). As a consequence, the SO for AP 2 is higher. In a densely deployed LiFi network, the SO will have such an impact that in these conditions, AP 2 will provide a better signal. This is shown in Table II, where the average channel gain and SO are multiplied to obtain the overall gain, that accounts for both the channel gain and the SO (and consequently, the PS effect). As it can be seen, the PS effect cannot be overlooked in this kind of scenario, and if the average AoI is known, calculating the SO can be useful to

estimate its impact. Fig. 6 show a comparison of Monte Carlo simulations for the SO $W(\psi)$ for both APs, which are also compared with a fitted Gaussian distribution. These suggest that the SO is following a similar distribution as the polar angle (θ), although this should still be confirmed experimentally. More importantly, these results show that AP 2 has a better overlap, and that the PS effect is completely compensating the difference in the channel gain between the 2 APs. Exploiting prior knowledge on the polar angle distribution of the device (and thus the AoI) in the envisioned application, a specific system design choice can be made with respect to where the CWL of the receiver OF is placed, so that the SO is maximised for that specific AoI. Another (and possibly more fruitful) way of taking advantage of the PS effect, is to employ a dynamic channel allocation that makes use of the internal sensors of the device, and access the information regarding its polar angle. In this way, it would be possible to estimate the SO and make a decision regarding which transmitter-receiver colour combination has the best overlap at that specific AoI, thus increasing the signal strength and improving the network capacity with respect to a fixed allocation. Results of this latter approach have been presented and discussed in [14], and the interested reader will thereby find a detailed description of what the benefits are in terms of improved fairness, network capacity and reduced link outage probability.

VI. Conclusions

In this paper, the impact of the PS phenomenon in OWC and LiFi networks employing WD has been discussed. First a mathematical framework has been set for its analysis, then it has been shown the importance of considering the balance between the channel gain and the SO, and design a system that is able to account for both of these parameters. It has been shown that in a densely deployed LiFi network employing WD, the SO cannot be neglected as its contribution is an important part of the final gain. Especially if user mobility is a requirement, leveraging this parameter can lead to improved system performances. One possible direction for a future study, as previously stated, is that of finding a closed form approximation for the SO presented in Equation (12). This would be useful in the practical implementation of a dynamic channel allocation strategy. Finally, as one of the key aspects in the adoption of LiFi is interference mitigation, another possible direction for a future study is to investigate what the contribution of both these parameters is on the interference, so that better strategies can be envisioned and implemented.

Acknowledgment

This work has been funded by the European Union's Horizon 2020 research and innovation programme under the Marie Skłodowska Curie grant agreement ENLIGHT'EM No. 814215.

References

[1] I. Demirkol, D. Camps-Mur, J. Paradells, M. Combalia, W. Popoola, and H. Haas, "Powering the internet of things through light communication," *IEEE Communications Magazine*, vol. 57, no. 6, pp. 107–113, 2019.

[2] O. Alsulami, A. Alahmadi, S. Saeed, S. Mohamed, T. El-Gorashi, M. Alresheedi, and J. Elmirghani, "Optimum resource allocation in 6g optical wireless communication systems," 05 2020. © 2020 IEEE.

[3] B. Marr, "Will lifi take big data and the internet of things to a new level?." https://www.forbes.com/sites/bernardmarr/2016/01/12/will-lifi-take-big-data-and-the-internet-of-things-to-a-new-level/, 01 2016.

[4] S. R. Teli, S. Zvanovec, and Z. Ghassemlooy, "Optical internet of things within 5g: Applications and challenges," in *2018 IEEE International Conference on Internet of Things and Intelligence System (IOTAIS)*, pp. 40–45, 2018.

[5] A. Gupta and X. Fernando, "Exploring secure visible light communication in next-generation (6g) internet-of-things," in *2021 International Wireless Communications and Mobile Computing (IWCMC)*, pp. 2090–2097, 2021.

[6] M. Z. Chowdhury, M. K. Hasan, M. Shahjalal, M. T. Hossan, and Y. M. Jang, "Optical wireless hybrid networks: Trends, opportunities, challenges, and research directions," *IEEE Communications Surveys Tutorials*, vol. 22, no. 2, pp. 930–966, 2020.

[7] M. D. Soltani, A. A. Purwita, Z. Zeng, H. Haas, and M. Safari, "Modeling the random orientation of mobile devices: Measurement, analysis and lifi use case," *IEEE Transactions on Communications*, vol. 67, no. 3, pp. 2157–2172, 2019.

[8] H. Haas, L. Yin, Y. Wang, and C. Chen, "What is lifi?," *Journal of Lightwave Technology*, vol. 34, no. 6, pp. 1533–1544, 2016.

[9] H. Haas, "High-speed wireless networking using visible light." http://spie.org/x93593.xml, April 2013.

[10] "What is Internet of Things (IoT)?." https://internetofthingsagenda.techtarget.com/definition/Internet-of-Things-IoT. Accessed: 2021-09-10.

[11] R. Bian, I. Tavakkolnia, and H. Haas, "15.73 gb/s visible light communication with off-the-shelf leds," *Journal of Lightwave Technology*, vol. 37, no. 10, pp. 2418–2424, 2019.

[12] H. Chun, S. Rajbhandari, G. Faulkner, D. Tsonev, E. Xie, J. J. D. McKendry, E. Gu, M. D. Dawson, D. C. O'Brien, and H. Haas, "Led based wavelength division multiplexed 10 gb/s visible light communications," *Journal of Lightwave Technology*, vol. 34, no. 13, pp. 3047–3052, 2016.

[13] J. Senior, S. Cusworth, and A. Ryley, "Wavelength division multiple access in fibre optic lans," in *IEE Colloquium on Fibre Optic LANS and Techniques for the Local Loop*, pp. 5/1–5/4, 1989.

[14] G. L. Martena, R. Bian, and H. Haas, "Adaptive wdma: Improving the data rate of a densely deployed lifi network," in *Proceedings of the Workshop on Internet of Lights*, IoL '21, (New York, NY, USA), p. 7–12, Association for Computing Machinery, 2021.

[15] P. Ge, X. Liang, J. Wang, C. Zhao, X. Gao, and Z. Ding, "Optical filter designs for multi-color visible light communication," *IEEE Transactions on Communications*, vol. 67, no. 3, pp. 2173–2187, 2019.

[16] P. Ge, X. Ling, J. Wang, X. Liang, R. Zhang, and C. Zhao, "Optical filter bank for multi-color visible light communications," in *2019 IEEE Global Communications Conference (GLOBECOM)*, pp. 1–6, 2019.

[17] P. Ge, X. Ling, J. Wang, X. Liang, S. Li, and C. Zhao, "Optical filter bank modeling and design for multi-color visible light communications," *IEEE Photonics Journal*, vol. 13, no. 1, pp. 1–19, 2021.

[18] M. Dehghani Soltani, A. A. Purwita, I. Tavakkolnia, H. Haas, and M. Safari, "Impact of device orientation on error performance of lifi systems," *IEEE Access*, vol. 7, pp. 41690–41701, 2019.

[19] J. Chen, I. Tavakkolnia, C. Chen, Z. Wang, and H. Haas, "The movement-rotation (mr) correlation function and coherence distance of vlc channels," *Journal of Lightwave Technology*, vol. 38, no. 24, pp. 6759–6770, 2020.

[20] M. Dehghani Soltani, A. A. Purwita, Z. Zeng, C. Chen, H. Haas, and M. Safari, "An orientation-based random waypoint model for user mobility in wireless networks," pp. 1–6, 2020.

[21] M. A. Arfaoui, M. D. Soltani, I. Tavakkolnia, A. Ghrayeb, C. M. Assi, M. Safari, and H. Haas, "Measurements-based channel models for indoor lifi systems," *IEEE Transactions on Wireless Communications*, vol. 20, no. 2, pp. 827–842, 2021.

[22] J. R. Barry and J. M. Kahn, "Link design for nondirected wireless infrared communications," *Appl. Opt.*, vol. 34, pp. 3764–3776, 07 1995.

[23] J. Kahn and J. Barry, "Wireless infrared communications," *Proceedings of the IEEE*, vol. 85, no. 2, pp. 265–298, 1997.